Calcium electrogenesis in distal apical dendrites of layer 5 pyramidal cells at a critical frequency of back-propagating action potentials

M. E. Larkum*, K. M. M. Kaiser, and B. Sakmann

Abteilung Zellphysiologie, Max-Planck-Institut für Medizinische Forschung, Jahnstrasse 29, D-69120 Heidelberg, Germany

Action potentials in juvenile and adult rat layer-5 neocortical pyramidal neurons can be initiated at both axonal and distal sites of the apical dendrite. However, little is known about the interaction between these two initiation sites. Here, we report that layer 5 pyramidal neurons are very sensitive to a critical frequency of back-propagating action potentials varying between 60 and 200 Hz in different neurons. Bursts of four to five back-propagating action potentials above the critical frequency elicited large regenerative potentials in the distal dendritic initiation zone. The critical frequency had a very narrow range (10–20 Hz), and the dendritic regenerative activity led to further depolarization at the soma. The dendritic frequency sensitivity was suppressed by blockers of voltage-gated calcium channels, and also by synaptically mediated inhibition. Calcium-fluorescence imaging revealed that the site of largest transient increase in intracellular calcium above the critical frequency was located 400–700 μm from the soma at the site for initiation of calcium action potentials. Thus, the distal dendritic initiation zone can interact with the axonal initiation zone, even when inputs to the neuron are restricted to regions close to the soma, if the output of the neuron exceeds a critical frequency.

The presence of two initiation zones in different regions of layer 5 (L5) pyramidal neurons (1) has interesting consequences for the integration of synaptic inputs arriving at these cells (for review, see ref. 2). Depolarization in the distal regions of the apical dendrite affects the neuron's firing behavior differently than somatic depolarization by evoking calcium action potentials (Ca^{2+}-APs) and bursts of somatic APs (3, 4). Back-propagating sodium APs (Na$^+$-APs) generated in the axon cause depolarization in the distal dendrites (5) and can interact with dendritic synaptic inputs to initiate Ca^{2+}-APs (4). In this way, synaptic inputs arriving at locations near the soma influence dendritic Ca^{2+} electrogenesis through the generation of Na$^+$-APs in the axon. Thus, it is important to understand the relationship between the APs initiated in the axon, the output of the neuron, and dendritic Ca^{2+} electrogenesis.

APs that back-propagate into the apical dendrite have been shown to cause Ca^{2+} influx in pyramidal neurons (1, 6–8). Bursts of APs have been linked to regenerative activity in the distal dendritic initiation zone (3, 4, 9, 10). During whisker stimulation, somatically recorded APs in L5 pyramidal neurons of the barrel field of the cortex can occur in high-frequency bursts, each consisting of 2–5 APs at 100–250 Hz (11). The degree of attenuation of the amplitude of back-propagating dendritic APs increases with increasing distance from the soma and depends on the frequency of APs (5). Single dendritic APs and low-frequency bursts of APs are attenuated strongly in the distal parts of the dendritic arbor (5, 12). Here, we explore the relationship between the frequency of APs generated in the axon and regenerative activity in the dendrite. The results show that dendritic Ca^{2+} electrogenesis is highly frequency-sensitive to back-propagating APs.

Materials and Methods

Slice Preparation. Experiments were performed in somatosensory neocortical slices from adult (28–57 days old) Wistar rats ($n =$ 33). The rats were deeply anesthetized by halothane and decapitated. The brain was quickly removed into cold (0–4°C), oxygenated physiological solution containing: 125 mM NaCl, 2.5 mM KCl, 1.25 mM NaH$_2$PO$_4$, 25 mM NaHCO$_3$, 1 mM MgCl$_2$, 25 mM dextrose, and 2 mM CaCl$_2$ (pH 7.4). Sagittal slices, 300 μm thick, were cut from the tissue block with a microslicer and kept at 37°C.

Electrophysiology. All experiments were performed at 34.0 ± 0.5°C with dual and triple recordings from single, identified L5 pyramidal neurons by using infrared illumination combined with differential interference contrast optics (13). Somatic (5–10 MΩ) and dendritic (10–25 MΩ) recording pipettes were filled with the standard intracellular solution containing: 105 mM potassium gluconate, 10 mM Hepes, 4 mM MgATP, 0.3 mM GTP, 30 mM KCl, and 2% biocytin (pH 7.3). Whole-cell recordings were made with up to three Axoclamp-2B amplifiers (Axon Instruments, Foster City, CA). Somatic-current injection was made with brief (2–5 ms) pulses in trains of 4–5 APs at frequencies ranging from 40 to 200 Hz. The measurement of additional somatic depolarization at supracritical frequencies was made by finding the maximum difference in membrane potential at the somatic electrode 8–18 ms after the last AP in the train between sub- and supracritical frequency trains. γ-Aminobutyric acid (GABA)ergic synaptic stimulation was made with a bipolar electrode with three voltage pulses (100–200 μs, up to 5 V) at 200 Hz in the presence of 50 μM 6-cyano-7-nitroquinoxaline-2,3-dione and 200 μM 2-amino-5-phosphonovaleric acid in the external solution to block excitatory transmission. The stimulating electrode was typically placed in layer 2/3 or on the border with layer 1, about 500 μm lateral to the cells from which the recordings were made. After recordings, slices were fixed and stained as described previously (1) for later reconstruction. All results are reported as mean ± SEM.

Calcium Imaging. For optical recording of dendritic Ca^{2+} transients, we combined dual whole-cell recording with Ca^{2+} imaging. Neurons were loaded with a Ca^{2+} fluorescence indicator (250 μM fura-2), which was added to the standard internal solution in both somatic and dendritic pipettes. Fluorescence changes were detected with a back-illuminated frame-transfer charge-coupled device camera (Princeton Instruments, Trenton NJ). Regions of interest (typically 5–15 × 3 μm) were selected on the dendrites (apical, apical oblique, and basal dendrites) at different locations from the soma. Fluorescence signals were converted to Ca^{2+} concentrations by using the standard ratioing equations (6, 14).

Results

Critical AP Frequency. We made simultaneous dual and triple whole-cell voltage recordings from the soma and apical dendrite of L5 pyramidal neurons of rat neocortex (Fig. 1A). APs were elicited in the axon (5) by 2- to 5-ms square-pulse current injection at the soma at a series of frequencies in steps of 10 Hz (Fig. 1 B and C, bottom traces). At lower frequencies (<98 ± 6 Hz, n = 31), the amplitude of four successive APs recorded at the distal dendritic site (665 ± 15 μm from soma, n = 24) remained the same or decreased in amplitude and duration (Fig. 1B, top trace). Above a particular frequency, referred to as the "critical frequency" (98 ± 6 Hz, median = 90 Hz, n = 31 of 33), successive APs recorded at the distal dendritic site increased substantially in amplitude and/or duration (Fig. 1C, top trace). At the proximal apical dendrite (336 ± 23 μm from soma, n = 12), the APs did not increase significantly in amplitude but did broaden considerably at supracritical frequencies (Fig. 1 B and C, middle traces). The activation of the distal dendritic regenerative potential above the critical frequency was reflected at the soma in the slower time course of repolarization after the last AP in a burst (Figs. 1C and 3B, arrows). The supracritical dendritic regenerative activity resulted in an additional depolarization [8 ± 1 mV; n = 23; range 3–17 mV (see *Materials and Methods*)] at the soma, which was sufficient to cause an additional AP in five neurons.

The membrane potential of the fourth AP in the train recorded at the distal dendritic site (Fig. 2A) usually exceeded 0 mV (+1.9 mV ± 1.7 mV, n = 26) at the critical frequency. The first AP recorded at the distal site varied in amplitude from cell

to cell (29.7 ± 3.8 mV, n = 26, range 5–75 mV), whereas above the critical frequency, the last AP always had a large amplitude (58.9 ± 1.6 mV, n = 26, range 38–72 mV). When the first AP was already large, the increase in amplitude of successive APs in the dendrite was less pronounced. However, substantial broadening of the successive APs was observed in all neurons. Thus, a more sensitive measure of dendritic regenerative activity was the time integral of membrane potential (V_m) for the four APs (Fig. 2B, shaded areas) positive to the resting potential. In this way, the critical frequency was determined by the sharp increase in the integral of V_m when plotted against AP frequency (Fig. 2C). When the critical frequency was reached, the integral almost doubled from 0.70 ± 0.07 mV·s to 1.32 ± 0.09 mV·s (n = 26). The critical frequencies determined with this method were mostly between 70 and 100 Hz (Fig. 2D), with the distribution skewed toward higher frequencies. No cell had dendritic regenerative activity at frequencies <60 Hz.

Calcium Dependence. As the frequency of the APs was increased above the critical frequency, the last two APs recorded at the distal dendritic site tended to merge (Fig. 2B) and resembled the distal dendritic Ca^{2+}-AP observed previously in these neurons (1). It was abolished by the addition of voltage-gated Ca^{2+} channel blockers [Cd^{2+} (50 μM) and/or Ni^{2+} (100 μM), n = 10] to the external solution. Fig. 3A shows the recording configuration with a distal dendritic recording site. The critical frequency was 90 Hz for this neuron (Fig. 3B, solid lines). The voltage–time integral at this frequency was 1.52 mV·s compared with 0.38 mV·s at 80 Hz (Fig. 3B, dotted line). After the addition of Cd^{2+}, the last two APs at 90 Hz were reduced to amplitudes recorded at subcritical frequencies (Fig. 3C), and the voltage integral was reduced to 0.58 mV·s at 90 Hz. The effect of crossing the critical frequency could also be blocked by the addition of 100 μM Ni^{2+} (n = 3), suggesting that the activation was determined by the combined influence of both high and low voltage-activated Ca^{2+} channels (15). Interestingly, the amplitude of the second AP in the train increased even in the presence of Cd^{2+}. This suggests that the mechanism underlying the frequency-dependent increase in the amplitude of the second AP of a train does not depend on voltage-gated Ca^{2+} channels.

GABAergic Inhibition. The dendritic Ca^{2+}-AP can be blocked by GABAergic inhibition (4). Here, we show that the dendritic frequency sensitivity to back-propagating APs is blocked by an inhibitory postsynaptic potential (IPSP) evoked by a single inhibitory neuron (Fig. 4A). The IPSP was generated by delivering eight somatic current pulses (at 200 Hz) to an inhibitory neuron located at the border between layers 2/3 and 4. This neuron was connected to a pyramidal neuron from which we recorded at the soma and a distal dendritic site (700 μm from the soma). At supracritical frequencies (here 100 Hz) the back-propagating APs recorded at the dendritic site merged to form a potential wave form resembling a Ca^{2+}-AP (Fig. 4B). This potential was blocked when the train of APs in the pyramidal neuron was preceded by an inhibitory input (Fig. 4C) revealing the underlying back-propagating APs. This blocking effect could also be demonstrated by using an extracellular stimulation electrode placed on the border of layers 1 and 2 to generate a compound IPSP in the pyramidal neuron in the presence of 50 μM 6-cyano-7-nitroquinoxaline-2,3-dione and 200 μM 2-amino-5-phosphonovaleric acid in the extracellular solution to block excitatory transmission (n = 9). Under such conditions, the dendritic regenerative activity due to high frequency back-propagating APs could be blocked by an extracellularly evoked IPSP occurring up to 400 ms before the train of APs. Inhibition did not have a significant effect on the amplitude of back-propagating Na^+-APs [in contrast to
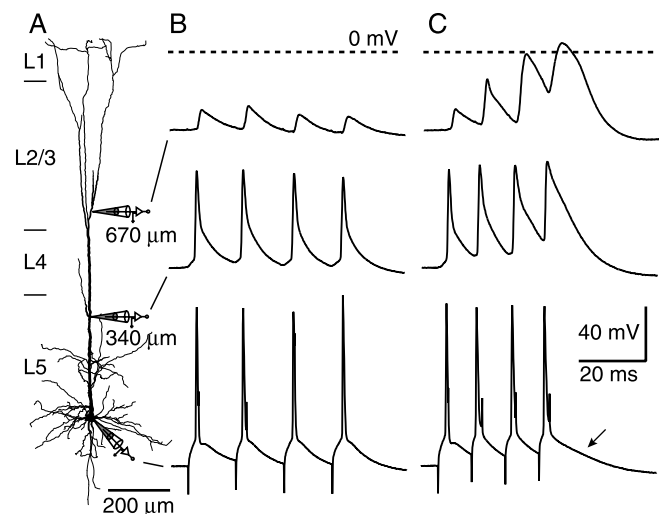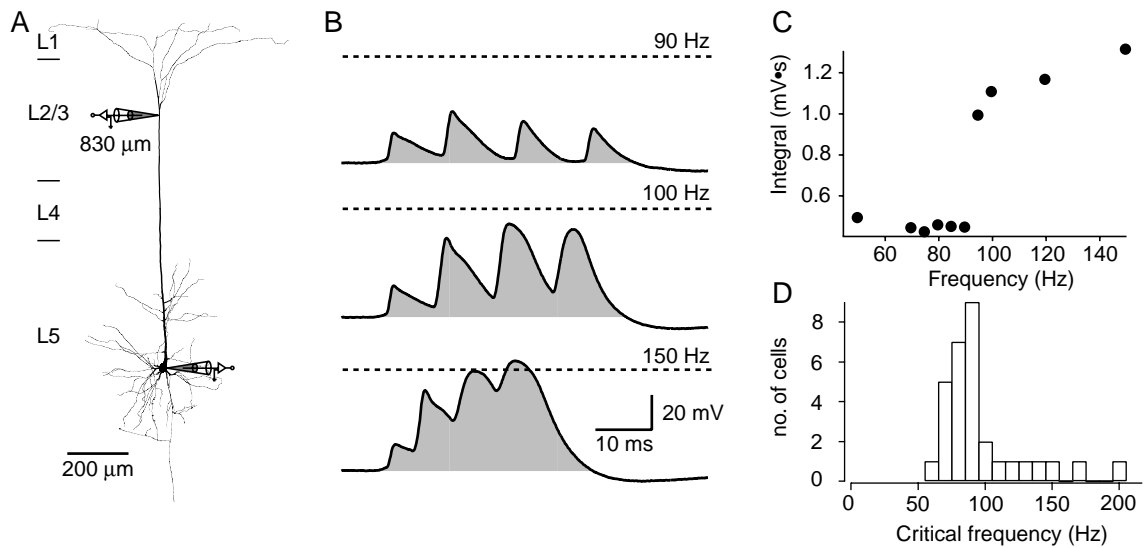

Fig. 1. Critical frequency for back-propagating APs that lead to regenerative potentials in the apical dendrites of a L5 pyramidal neuron. (A) Recording configuration. Triple whole-cell voltage recording from a pyramidal neuron in an acute slice of neocortex from a 34-day-old rat. The neuron was filled with biocytin during the experiment and later reconstructed. The most distal recording pipette was placed 670 μm from the soma, and another pipette was placed at the proximal apical dendrite, 340 μm from the soma. (B) A train of square-pulse current injections at the soma at 70 Hz elicited back-propagating APs that decreased in amplitude substantially by 670 μm, although the attenuation was small in the proximal apical dendrite. (C) When the frequency of the APs elicited at the soma was high enough (here 100 Hz), the distal dendritic voltage response was substantially altered. The amplitude and duration of each successive dendritic AP increased by up to 4-fold. Only lengthening was apparent in the proximal apical dendrite, and the somatic response was almost indistinguishable from subcritical frequencies, except for a brief time interval 8–18 ms after the last AP, in which there was a maximum additional 9 mV depolarization (arrow). The dashed lines represent 0 mV for the distal dendritic recording.

Fig. 2. Voltage integral as a measure of critical frequency across neurons. (*A*) Reconstruction of a biocytin-filled L5 pyramidal neuron from a 57-day-old rat with a dendritic whole-cell patch pipette located 830 μm from the soma and a second pipette located at the soma. (*B*) Four 5-ms square-pulse current injections at the soma at 90 Hz (top trace) elicited APs at the soma that had amplitudes of approximately 20–30 mV recorded at the dendritic site. The shaded region represents the voltage time integral, which had a value of 0.50 mV·s. At the critical frequency, 100 Hz (middle trace), the integral increased to 1.28 mV·s. At 150 Hz (bottom trace), the V_m crossed 0 mV, but the integral did not greatly increase. The dashed lines represent 0 mV. (*C*) The integral of four successive APs over time at different frequencies in the same neuron shows a sharp nonlinear increase at the critical frequency. (*D*) The critical frequencies of 31 different L5 pyramidal neurons. The average value was 98 ± 6 Hz, but the distribution was skewed toward higher values. In two cells, no detectable critical frequency was reached below 200 Hz (data not shown).

hippocampal CA1 pyramidal cells (16)], except at very high stimulus intensity.

Calcium Accumulation. High-frequency back-propagating APs can elicit regenerative activity that resembles a Ca^{2+}-AP in the distal dendrites. However, because it involves a train of APs that back-propagate along the dendrite and activate voltage-gated Ca^{2+} channels along the length of the apical dendrite (7), it

remained an open question as to whether the change in intracellular calcium concentration ($\Delta[Ca^{2+}]_i$) along the dendrite had a similar distribution as that when a Ca^{2+}-AP was elicited by current injection in the dendrite (1). We therefore imaged changes in dendritic $[Ca^{2+}]_i$ evoked by back-propagating APs at sub- and supracritical frequencies by using a Ca^{2+} indicator (Fig. 5).

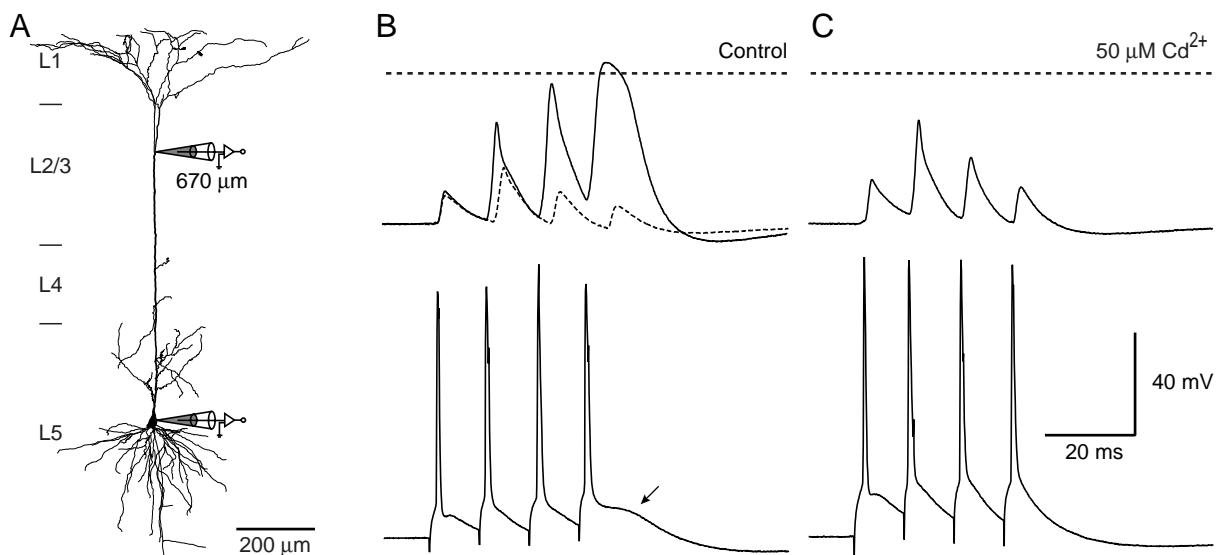Pipettes filled with fura-2 (250 μM) were used to record

Fig. 3. Calcium-dependent regenerative potential at the critical frequency. (*A*) Reconstruction of a biocytin-filled L5 pyramidal neuron from a 33-day-old rat with a dendritic whole-cell patch pipette located 670 μm from the soma and a second pipette located at the soma. (*B*) Control response recorded at the dendritic site (top trace) at the critical frequency (90 Hz, solid line) and subcritical frequency (80 Hz, dashed line). A small depolarization was observable at the soma (arrow, bottom trace; 90 Hz) corresponding to the fourth broad AP recorded at the dendritic site. (*C*) After the addition of the voltage-sensitive calcium channel blocker Cd^{2+} (50 μM), the response recorded at both sites was similar to the response at subcritical frequencies. The effect was largest on the last two APs in the train, with only a slight reduction in the duration of the second AP, suggesting that the increase in amplitude of the second AP is not dependent on Ca^{2+} influx. The horizontal dashed lines represent 0 mV at the dendritic recording.
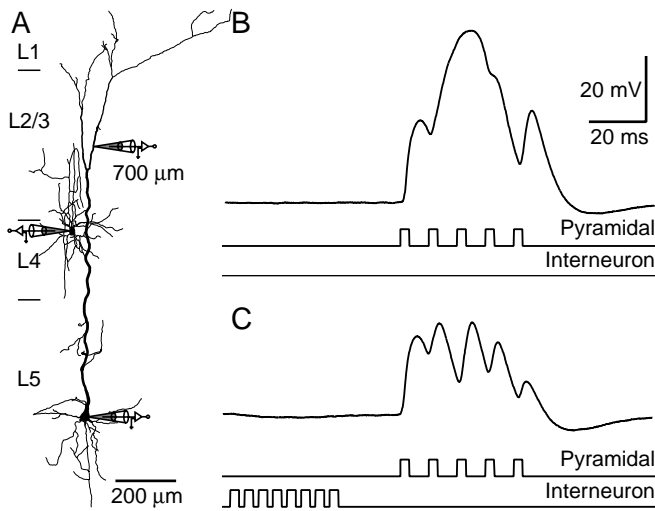
Fig. 4. GABAergic input blocks the Ca^{2+} component of the dendritic response above the critical frequency. (*A*) Reconstruction of a biocytin-filled L5 pyramidal neuron and an interneuron located at the top of layer 4 that innervated the pyramidal neuron. The rat was 49 days old. A dendritic whole-cell recording pipette was located 700 μm distal to the soma, and another pipette was located at the soma. (*B*) Dendritic potential in response to a supracritical train of APs (100 Hz) elicited at the soma of the pyramidal neuron. The two bottom traces represent schematically the time course of the current injected at the somata of both neurons. (*C*) The regenerative potential in the dendrite was blocked in a manner similar to the block due to extracellular Cd^{2+} (50 μM), when a compound IPSP, generated by eight APs elicited in the presynaptic neuron (200 Hz), preceded the pyramidal cell stimulation.

were chosen along the apical dendrite (and in some cells on the basal and apical oblique dendrites as well). During subcritical frequency trains of back-propagating APs, the change in [Ca^{2+}]$_i$ rose substantially near the soma, basal dendrites (data not shown), and proximal apical dendrites, but failed to make large changes in the distal apical dendrites (Fig. 5*B*, 80 Hz). However, above the critical frequency, the peak Δ[Ca^{2+}]$_i$ suddenly rose to levels comparable to the soma (Fig. 5*B*, 100 Hz). This frequency sensitivity of dendritic [Ca^{2+}]$_i$ transients corresponded precisely to the critical frequency for the voltage integral, as measured at the distal dendritic site ($\approx$600 μm; Fig. 5 *C* and *D*). The peak Δ[Ca^{2+}]$_i$ at all regions is plotted as a function of back-propagating AP frequency in Fig. 5*E* (●). The voltage integral recorded at the dendritic site (○) is superimposed and shows a close correspondence to Δ[Ca^{2+}]$_i$ at the imaged region of interest that was closest to the dendritic pipette (region 4).

In 10 of 12 neurons, the dendritic region of largest peak Δ[Ca^{2+}]$_i$ was between 400 and 700 μm from the soma. In one neuron (the only intrinsically bursting neuron we found), the region with the largest peak in Δ[Ca^{2+}]$_i$ was located 200 μm from the soma, although the distal regions also showed large changes in [Ca^{2+}]$_i$. At the soma and in the basal dendrites, the rise in Δ[Ca^{2+}]$_i$ was a linear function of frequency. In one additional neuron, no critical frequency could be detected as the Δ[Ca^{2+}]$_i$ rose steadily at each successive step in frequency. In all neurons, a supralinear increase in dendritic V$_m$ at the critical frequency was reflected in a concomitant supralinear increase in Δ[Ca^{2+}]$_i$ in the distal apical dendrite. We therefore concluded that the Ca^{2+} current in the distal dendrite evoked by supracritical frequency back-propagating APs is very similar to the Ca^{2+} current during a Ca^{2+}-AP evoked by dendritic current injection (1).

Discussion

The results indicate that each L5 pyramidal neuron is very sensitive to a critical frequency of Na$^+$-APs. The frequency

simultaneously from pyramidal cells at both the soma and the distal apical dendrite (Fig. 5*A*). Regions of interest for imaging
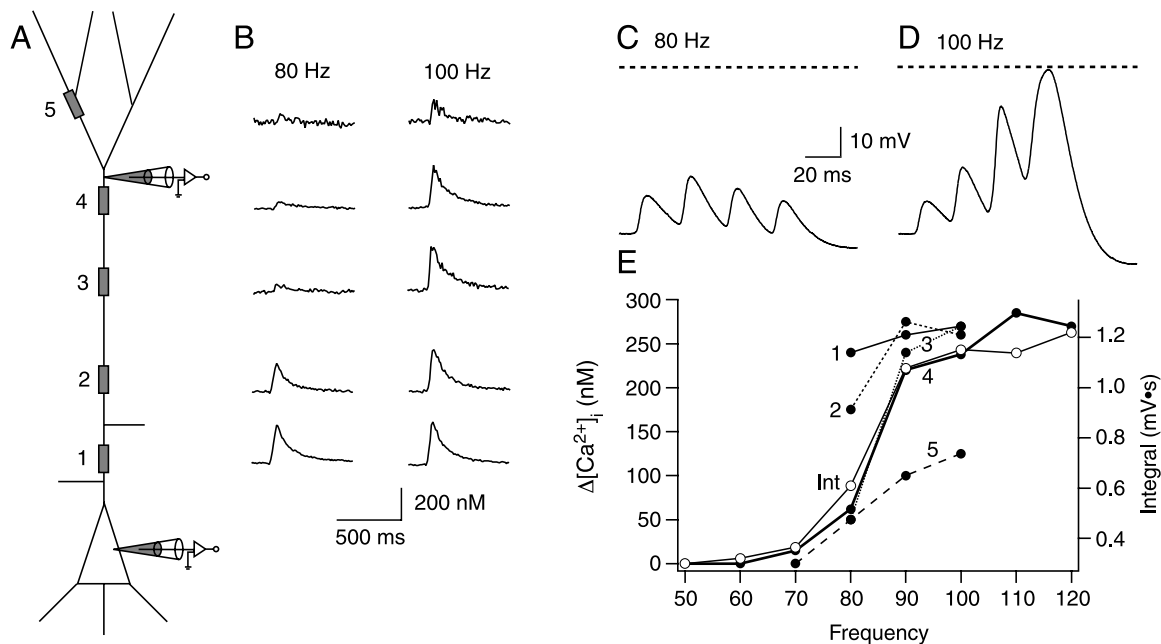

Fig. 5. Imaging dendritic calcium transients during high-frequency stimulation. (*A*) Schematic representation of an L5 pyramidal neuron showing the dendritic voltage recording at $\approx$600 μm from the soma and at the soma. The gray boxes indicate regions of interest chosen for imaging calcium fluorescence transients; regions 1–5 were 50, 200, 400, 600, and 800 μm from soma, respectively. (*B*) Dendritic [Ca^{2+}]$_i$ transients evoked by four somatically elicited APs below the critical frequency (80 Hz, *Left*) and above the critical frequency (100 Hz, *Right*). The traces are placed beside the corresponding recording sites shown in *A*. Electrical response recorded at the dendritic pipette at 80 Hz (subcritical) (*C*) and 90 Hz (supra-critical) (*D*). The dashed lines represent 0 mV. (*E*) Peak Δ[Ca^{2+}]$_i$ recorded in the each of the five regions shown in *A* (●). The time integral (Int) of the voltage response recorded at the dendritic site is also shown (○). Its frequency dependence corresponds closely to that of Δ[Ca^{2+}]$_i$ recorded at region 4 (closest to the dendritic recording pipette).

range where the activation of the dendritic initiation zone usually occurs is between 70 Hz and 100 Hz, but its exact value is different for each neuron and can sometimes be as high as 200 Hz.

The mechanism underlying the frequency sensitivity is related to summation of back-propagating APs in the distal dendrite. When the APs summate to reach threshold for a Ca^{2+}-AP, the regenerative properties of the distal initiation zone dominate the dendritic membrane potential. The initial depolarization must be prolonged, however, which is evident from the fact that single back-propagating APs often cross the threshold for a Ca^{2+}-AP for a short time without eliciting a Ca^{2+}-AP. Furthermore, the situation is complicated by the fact that successive dendritic APs tend to decrease in amplitude at low frequencies (5), as in hippocampal pyramidal neurons (12), but, as we show here, increase in amplitude close to and above the critical frequency. We found that the amplitude of the first back-propagating AP varied from cell to cell, as also observed *in vivo* (17, 18). However, it was the frequency of the train of back-propagating APs, not their amplitudes, that was critical for the generation of a dendritic Ca^{2+}-AP. This also suggests that the major determinant for the initiation of dendritic Ca^{2+} electrogenesis was the duration of the depolarization rather than the amplitude.

The dendritic AP threshold can be reduced by a single back-propagating AP (4). Here, we demonstrate that no distal input at all is necessary for the activation of the distal dendritic initiation zone under certain conditions. It should also be pointed out that, at frequencies just below the critical frequency, the effectiveness of distal dendritic input is at a maximum. This could be demonstrated by combining a subthreshold excitatory postsynaptic potential-like current injection into the dendrite with subcritical frequency back-propagating APs that then generated a Ca^{2+}-AP ($n = 6$; data not shown). This indicates that the AP activity of a pyramidal neuron can itself become a mechanism for "priming" its responsiveness to distal dendritic input. Thus, as the neuron becomes more active, the efficacy of inputs to the dendritic tree is redistributed.

The location of the largest change in $[Ca^{2+}]_i$ corresponded to the site where there was the greatest change in V_m, i.e., the site of initiation of Ca^{2+}-APs. We therefore concluded that a train of back-propagating APs was evoking a Ca^{2+}-AP. Nonetheless, the distribution of $[Ca^{2+}]_i$ along the apical dendrite was slightly different from the distribution of $[Ca^{2+}]_i$ following Ca^{2+}-APs evoked by dendritic current injection alone (1) in that the train of back-propagating APs also caused $[Ca^{2+}]_i$ increases along the proximal apical dendrite. Even subcritical frequency trains of back-propagating APs caused a large Ca^{2+} influx along the first few hundreds of micrometers of the apical dendrite (Fig. 5B) but not in regions more distal than about 400 μm from the soma. The result was that the $[Ca^{2+}]_i$ distribution following a suprathreshold train of APs included a significant change in the $[Ca^{2+}]_i$ profile in the proximal apical dendrite that was the result of the back-propagating APs rather than Ca^{2+} regenerative activity in the distal apical initiation zone.

As with Ca^{2+}-APs evoked by dendritic current injection, Ca^{2+} regenerative activity evoked by high-frequency back-propagating APs was also very sensitive to GABAergic inhibition. This implies that frequency-sensitive dendritic regenerative potentials can be restricted to certain areas of the cortex. In fact, a single bursting interneuron can alter the frequency sensitivity of a pyramidal neuron for hundreds of milliseconds. This suggests that, under normal circumstances with background inhibition (19), the firing pattern of pyramidal neurons will depend mostly on the integrative properties in the axon until inhibition is released for long enough for the dendritic initiation zone to contribute to axonal AP generation. The powerful effect of inhibition on dendritic regenerative activity during bursting has already been demonstrated in neocortical pyramidal neurons (4, 9) and in hippocampal pyramidal neurons (10, 20).

In summary, we have shown that neocortical pyramidal cells are very sensitive to the frequency of axonic Na^+-APs, with critical frequencies usually between 70 Hz and 100 Hz. When this critical frequency is reached, there is a sharp rise in dendritic $[Ca^{2+}]_i$ and a prolonged dendritic depolarization, which could lead to changes in the integrative properties of the neuron and affect Ca^{2+}-dependent metabolic processes in the distal dendrites.

1. Schiller, J., Schiller, Y., Stuart, G. & Sakmann, B. (1997) *J. Physiol. (London)* **505,** 605–616.
2. Rhodes, P. A. (1999) in *Cerebral Cortex*, eds. Ulinski, P. & Jones, E. G. (Plenum, New York), Vol. 13, pp. 139–200.
3. Schwindt, P. & Crill, W. (1999) *J. Neurophysiol.* **81,** 1341–1354.
4. Larkum, M. E., Zhu, J. J. & Sakmann, B. (1999) *Nature (London)* **398,** 338–341.
5. Stuart, G., Schiller, J. & Sakmann, B. (1997) *J. Physiol. (London)* **505,** 617–632.
6. Helmchen, F., Imoto, K. & Sakmann, B. (1996) *Biophys. J.* **70,** 1069–1081.
7. Markram, H., Helm, P. J. & Sakmann, B. (1995) *J. Physiol. (London)* **485,** 1–20.
8. Magee, J., Hoffman, D., Colbert, C. & Johnston, D. (1998) *Annu. Rev. Physiol.* **60,** 327–346.
9. Kim, H. G., Beierlein, M. & Connors, B. W. (1995) *J. Neurophysiol.* **74,** 1810–1814.
10. Buzsáki, G., Penttonen, M., Nádasdy, Z. & Bragin, A. (1996) *Proc. Natl. Acad. Sci. USA* **93,** 9921–9925.
11. Zhu, J. J. & Connors, B. W. (1999) *J. Neurophysiol.* **81,** 1171–1183.
12. Spruston, N., Schiller, Y., Stuart, G. & Sakmann B. (1995) *Science* **268,** 297–300.
13. Dodt, H. U. (1993) *Adv. Exp. Med. Biol.* **333,** 245–249.
14. Grynkiewicz, G., Poenie, M. & Tsien, R. Y. (1985) *J. Biol. Chem.* **260,** 3440–3450.
15. Avery, R. B. & Johnston, D. (1986) *J. Neurosci.* **16,** 5567–5582.
16. Tsubokawa, H. & Ross, W. N. (1996) *J. Neurophysiol.* **76,** 2896–2906.
17. Buzsáki, G. & Kandel, A. (1998) *J. Neurophysiol.* **79,** 1587–1591.
18. Kamondi, A., Acsády, L. & Buzsáki, G. (1998) *J. Neurosci.* **18,** 3919–3928.
19. Paré, D., Shink, E., Gaudreau, H., Destexhe, A. & Lang, E. (1998) *J. Neurophysiol.* **79,** 1450–1460.
20. Miles, R., Toth, K., Gulyas, A. I., Hajos, N. & Freund, T. F. (1996) *Neuron* **16,** 815–823.